$$v_1(\xi)=\begin{cases}1-\dfrac{2}{(\nu_3-\nu_2)(1-\sigma)}\left[\dfrac{\tilde{K}\tilde{q}(\gamma-1)}{\nu_3}+\tilde{K}+\dfrac{\tilde{q}(\gamma-1)^2}{\gamma}\right]e^{\nu_3\xi}, & \xi<0,\\ -1+\dfrac{2}{(\nu_2-\nu_3)(1-\sigma)}\left[\dfrac{\tilde{K}\tilde{q}(\gamma-1)}{\nu_2}+\tilde{K}+\dfrac{\tilde{q}(\gamma-1)^2}{\gamma}\right]e^{\nu_2\xi}, & \xi>0,\end{cases}$$

$$\tau_1(\xi)=\begin{cases}-1+\dfrac{\nu_3}{\nu_3+\tilde{q}(\gamma-1)}(1-v_1), & \xi<0,\\ 1-\dfrac{\nu_2}{\nu_2+\tilde{q}(\gamma-1)}(1+v_1), & \xi>0,\end{cases}$$

where $\nu_2 < 0$ or $\nu_3 > 0$ are roots of Eq. (4.4) at $\sigma < 1$.

The qualitative behavior of the functions $v_i(\xi)$, $\tau_i(\xi)$ as $\mu_i \to 0$ is shown in Fig. 4a, b for the cases $\sigma > 1$ and $\sigma < 1$ respectively. Thus, in the case of a low concentration of the heavy component (Fig. 4a) the mixture is in equilibrium right up to the shock wave front, after which the velocity and temperature of the heavy component relax to equilibrium values with no discontinuity. The heavy component temperature distribution in the shock wave is nonmonotonic. With a low concentration of the light component the mixture on both sides of the shock transition is in nonequilibrium conditions, tending to equilibrium as $\xi \to \pm\infty$. The temperature and velocity profiles of the light component are nonmonotonic.

LITERATURE CITED

1. G. A. Ruev, V. M. Fomin, and N. N. Yanenko, "Shock wave structure in gas mixtures," Dokl. Akad. Nauk SSSR, 261, No. 2 (1981).
2. V. V. Struminskii, "Effect of diffusion velocity on gas mixture flow," Prikl. Mat. Mekh., 38, No. 2 (1974).

SPALL DAMAGE TO A LIQUID METAL ACCOMPANYING PULSED ACTION OF RADIATION

S. N. Kolgatin, A. M. Stepanov, and
A. V. Khachatur'yants

UDC 532.595.2

The study of spallation accompanying the appearance of short-duration tensile stresses in a material, exceeding the material's tensile strength, is widely used to investigate the dynamic strength of solids [1]. Such stresses appear, in particular, in the presence of thermal shocks — pulsed volume liberation of energy in a material accompanying pulse durations t_p satisfying the condition $t_p \lesssim l/c$, where l is the characteristic size of the region of energy liberation and c is the velocity of sound in the material. As shown in [2], instantaneous thermal shocks (corresponding to the more stringent condition $t_p \ll l/c$), can lead to spalls with energy inputs significantly lower than the heat of fusion and, especially, the heat of evaporation of the material. In experiments modeling thermal shocks, laser radiation is usually used as the course of energy liberation for weakly absorbing media and relativistic electron beams (REB) are used for metals [3, 4]. Experiments with REB correspond, as a rule, to the weaker condition $t_p \lesssim l/c$.

Negative stresses and spalls can be observed not only in solids, but also in liquid metals [4]. The possibility of spalls must be taken into account, in particular, in setting up liquid-metal shielding of the first wall of pulsed thermonuclear reactors [5]. The action of fluxes of charged particles and x-ray radiation on a liquid metal usually leads to strong

Leningrad. Translated from Zhurnal Prikladnoi Mekhaniki i Tekhnicheskoi Fiziki, No. 5, pp. 55-59, September-October, 1984. Original article submitted July 17, 1983.

0021-8944/84/2505-0702$08.50

heating and evaporation of a thin surface layer and the formation of a shock wave, propagating into the bulk of the metal. The interaction of compression and unloading waves, their reflection from the wall or from the free surface of the liquid metal can cause significant negative pressures and ruptures of the liquid. These phenomena are studied in this work in the gas-dynamic approximation. The problem of the interaction of laser radiation with weakly absorbing dielectrics was studied in [6].

1. Working Model. We shall study a flat layer of liquid metal $0 \leqslant x \leqslant h$. A radiation flux with a surface energy density of $q_S(t)$ is incident on the metal surface (x = 0). The radiation energy is absorbed in the bulk of the metal according to the law

$$q_V = q_S \varkappa \exp\left(-\varkappa \int_0^x \rho(\xi)\, d\xi\right), \tag{1.1}$$

where $\varkappa = 1/\rho_0 l$ is the mass coefficient of absorption (assumed to be constant); ρ_0 is the initial density of the metal; and, $q_S(t) = q_0 f(t)$. The law (1.1) describes well the absorption of photons in the x-ray and γ-ray ranges of the spectrum. The absorption of the energy of charged particles obeys more complicated laws, even for a normally incident flux of monoenergetic particles [7]. Nevertheless, the applicability of (1.1) is often justified for charged particles also. Thus, in [3], the inclusion of the real spectrum and angles of incidence of electrons on a target led to a law of energy absorption which is close to (1.1).

To calculate the pressures which appear in the liquid, the following system of equations of gas dynamics in a Lagrangian form is used:

$$\frac{\partial}{\partial \tau}\left(\frac{1}{\varphi}\right) = \frac{\partial u}{\partial s}; \tag{1.2}$$

$$\partial u/\partial \tau = -\partial \pi/\partial s; \tag{1.3}$$

$$\partial \varepsilon/\partial \tau = -\pi \partial u/\partial s + Qf(\tau)e^{-s}. \tag{1.4}$$

The system (1.2)-(1.4) is presented in dimensionless variables. Denoting the critical parameters of the state of the metal by the index *, we have

$$\pi = p/p_*, \quad \varphi = \rho/\rho_*, \quad \Theta = T/T_*, \quad u = v/\left(\sqrt{p_*/\rho_*}\right),$$

$$\varepsilon = \frac{E}{p_*/\rho_*}, \quad s = \varkappa m = \varkappa \int_0^x \rho(\xi)\, d\xi, \quad \tau = t\varkappa \sqrt{p_* \rho_*}, \quad Q = \frac{q_0}{\sqrt{p_*^3/\rho_*}},$$

where p is the pressure, ρ is the density, T is the temperature, E is the internal energy, and v is the velocity. The dimensionless form is achieved by eliminating from the parameters of the problem the coefficient of absorption , and for a specific metal the solution depends only on the parameters of the pulse, characterized by the constant Q and its envelope $f(\tau)$, which describes its shape as a function of time. For a triangular pulse, used in the calculations, it has the following form:

$$f(\tau) = \begin{cases} 1 - |1 - \tau/\tau_p|, & \tau \leqslant 2\tau_p, \\ 0, & \tau > 2\tau_p. \end{cases}$$

The initial conditions for the system (1.2)-(1.4) have the form

$$u(s, 0) = 0, \ \pi(s, 0) = \pi_0, \tag{1.5}$$
$$\varphi(s, 0) = \varphi_0, \ \varepsilon(s, 0) = \varepsilon_0.$$

The boundary condition

$$\pi(0, \tau) = 0 \tag{1.6}$$

is imposed on the irradiated surface x = 0 (s = 0), while on the surface x = h ($s = s_0$) either the condition (1.6) (a free surface) or the condition of contact with a rigid wall

$$u(s_0, \tau) = 0 \tag{1.7}$$

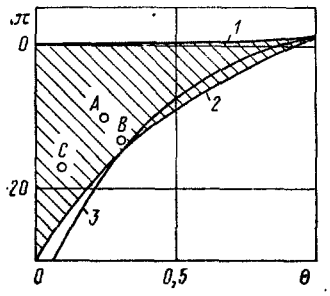

Fig. 1

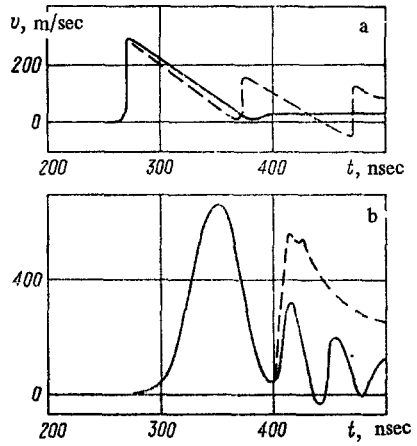

Fig. 2

is used. The problem (1.2)-(1.7) is closed by the equations of state and energy $\pi = \pi(\varphi, \Theta)$, $\varepsilon = \varepsilon(\varphi, \Theta)$, described in [8].

The pulsed character of energy liberation for durations $\sim 10^{-8}$ sec can lead both to overheating of the liquid relative to the equilibrium temperature of the phase transition $T_c(p)$ and to the appearance of negative pressures which are much lower than the equilibrium pressure $p_n(T)$. According to concepts of modern physics [9], the state of an expnaded liquid does not differ fundamentally from the state of an overheated liquid, and the limiting tensile stresses leading to rupture of the liquid can be estimated using the theory of homogeneous nucleation of the gas phase. Figure 1 shows the region of metastable states for liquid lithium in the π, Θ plane (the shaded region). Curve 1 is the boundary between the single- and two-phase states in thermodynamic equilibrium (binodal), curve 2 is the spinodal, calculated from the equations of state [8] from the condition for loss of thermodynamic stability $(\partial p/\partial \rho)_T = 0$, curve 3 is the limiting tensile strength of a liquid metal (for $\pi < 0$) or the limiting overheating of the metal (for $\pi > 0$), calculated using the Frenkel–Zel'dovich model of homogeneous nucleation [9]. It is evident that curves 2 and 3 determine practically the same limiting strength of the liquid.

Nonequilibrium states of the expanded liquid can appear when the condition $t_s \ll t_w$ holds, is satisfied, where t_s is the characteristic expansion time of the liquid in the unloading wave (usually close to the duration of the pulse t_p) and t_w is the average waiting time for the nucleus of the new phase [9]. As a rule, when the condition $t_p \lesssim l/c$, corresponding to a thermal shock, holds, the condition for a nonequilibrium state ($t_s \ll t_w$) also holds at the same time.

In contrast to this work, in [6] the time t_s is comparable not to the waiting time of a nucleus t_w, but to the time t_{st} for establishing a stationary rate of nucleation. It is thus assumed that the process of rupture of the material is determined not by the appearance of the first nuclei, but rather by their intense formation at a maximum rate. Kondrat'ev et al. [6] assume here that the time of formation of the critical bubble and its growth to sizes comparable to the size of the region of negative pressures l_s does not exceed t_{st}. This assertion, however, is valid only for very small sizes l_s and, correspondingly, dimensions of the region of energy liberation l. Thus the estimates ([9], p. 57) for an overheated liquid near the boundary of intense nucleation give the values $t_{st} \sim 10^{-9} - 10^{-8}$ sec. At the same time, the rate of growth of the bubble cannot exceed the velocity of sound in the liquid c, which for $l \sim 10^{-4}$ m and $c \sim 10^3$ m/sec gives a growth time of $\sim 10^{-7}$ sec, i.e., greater than t_{st}.

Experimentally observed ruptures of a liquid occur in most cases in the presence of tensile stresses which are several times lower than the theoretical strength, which is explained by the existence of centers of the new phase in the bulk of the liquid or at boundaries with solid surfaces. In the experiment of [4], rupture in liquid mercury nevertheless occurred in the presence of stresses which were lower than the theoretical stresses by only 20-40%. It should also be noted that the irradiation of liquids by high-energy particles (for example, neutrons) leads to the appearance of centers of vaporization in the liquid and lowers the cavitation strength of the liquid [5]. Thus real rupturing stresses in a liquid can differ significantly from the theoretical values.

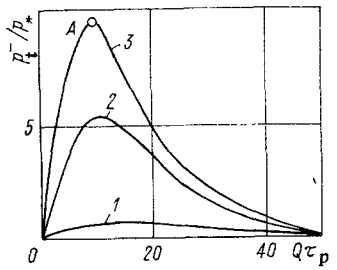

Fig. 3

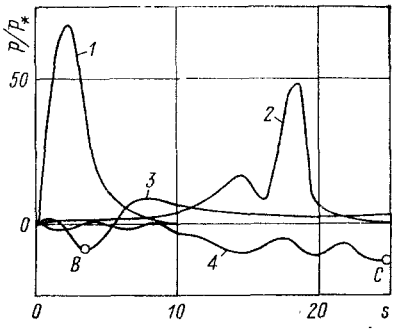

Fig. 4

The problem (1.2)-(1.7) was solved numerically with the help of a completely conservative implicit difference scheme [10].

2. Modeling of the Experiment in [4]. The problem was formulated as follows. A layer of mercury 0.25 mm thick was positioned between an aluminum plate (1.25 mm thick) and an acrylic plastic plate (5 mm thick). A high-current REB, incident on the outer surface of the aluminum plate, excited in it a compression pulse, which then penetrated into the mercury layer. The compression pulse was partially reflected from the mercury–plastic boundary and was partially converted into a tension pulse, just as on the free surface of a body (because of the much lower wave impedance of the Plexiglas than that of mercury). The displacement of the mercury–plastic boundary as a function of time was measured with the help of an interferometer, and the velocity of the boundary was measured from the displacement.

Figure 2a, taken from [4], shows the change in the velocity of the boundary as a function of time. It is evident that for some (threshold) value of the energy input in the pulse (1.5 MJ/m^2), anomalies appear in the behavior of the interface; for example, oscillations of its velocity are observed (dashed curve). In [4], this anomaly is attributed to the spallation of the liquid and the amplitude of the tensile stresses in mercury accompanying spallation is estimated to be 1900 MPa. Taking into account the fact that the rupture strength of mercury, according to the theory of homogeneous nucleation (in different approximations), is equal to 2300-3000 MPa, this experimental result (1900 MPa) may be regarded as a strong argument in support of this theory. We are not aware of other experimental studies, in which the rupture strengths of liquid metals which are as close to the theoretical values were achieved. For this reason, modeling of the experiment of [4], together with a check of the adequacy of the working model used, is also of interest in itself.

The calculation was performed for the conditions of an experiment in which spallation was observed (q_0 = 1.5 MJ/m^2, t_p = 30 nsec) using the equations of state of aluminum and mercury presented in [8]. The actual three-layer sample was replaced in the calculations by a two-layer sample (aluminum–mercury, taking into account their actual thicknesses). The outer mercury boundary was viewed as a free surface, i.e., the boundary condition (1.6) was used. It is natural that the spallation of mercury in this case leads not to oscillations of the boundary around the position of equilibrium, as in the experiment, but rather to flying off of the spalled layer. The results of the calculation are presented in Fig. 2b. The solid line shows the motion of the outer mercury boundary in the absence of spallation. It is evident that in contrast to the continuous curve with a single maximum in Fig. 2a, this curve has a sequence of humps and valleys. This indicates that the main compression wave is followed at the outer mercury boundary by secondary waves, which arise at the interface between the metals. After the main wave is reflected, a negative pressure with an amplitude of 2200 MPa appears near the mercury surface. If this value is taken as the rupture strength of mercury and the calculation is repeated, then the character of the motion of the outer mercury surface, after spallation, changes (dashed line in Fig. 2b). Satisfactory quantitative agreement between the calculation and the experiment is achieved with respect to the magnitudes of the negative pressures arising in the mercury. The disagreement in the time of onset of motion of the boundary can be explained by the fact that any delays in the measuring circuits were ignored and is not fundamental.

3. Numerical Experiment (for Lithium). Taking into account the thermodynamically nonequilibrium nature of the process, the computed pressure profile near the irradiated surface has the characteristic form of a compression pulse, propagating into the bulk of the metal, followed by an unloading wave, in which the pressures are negative, i.e., the liquid is stretched. The amplitude of the tension wave, after it is established, p_t^-, attained at a depth of $(1\text{-}2)l$, changes little thereafter. Thus conditions are created for spallation of the liquid from the front (toward the radiation). Figure 3 shows the dependence of the amplitude of the negative pressure at the front edge of the metal on the product $Q\tau_p$ (proportional to the energy input) and the dimensionless pulse duration τ_p ($\tau_p = 0.5$ for curve 1, $\tau_p = 0.1$ for curve 2, and $\tau_p = 0.01$ for curve 3). As the energy input is increased (with τ_p = const), the amplitude of the negative pressure grows, reaching a maximum at the value $Q\tau_p \sim 10$. The reason for the initial growth of p_t^- is quite obvious. The increase in the energy input leads to a growth of the amplitude of the compression wave forming near the wall and this, in its turn, increases the amplitude of the unloading wave. For sufficiently large energy inputs ($Q\tau_p > 10$), p_t^- near the irradiated surface begins to decrease. This is explained as follows. For energy inputs exceeding the binding energy of the atoms, the surface layer of the metal separates during the unloading accompanied by a severalfold decrease of the density. The elastic component of the pressure of the metal becomes small, and the separation of the surface layer does not appreciably affect the neighboring layers.

For lithium, $Q\tau_p \simeq 10$ corresponds to an energy input of 6.5 MJ/kg near the surface or an overheating of the lithium by $\Delta T = 1500°K$ (the critical parameters of lithium are: $p_* = 68.9$ MPa, $\rho_* = 105$ kg/m^3, and $T_* = 3223°K$). The magnitude of the maximum on the curves in Fig. 3 increases as the pulse duration decreases and reaches $\tau_p \lesssim 0.01$ for values of $\sim 10p_*$ (i.e., for an instantaneous thermal shock). The maximum tensile pressures appear at a depth of $x \sim 1.5l$, where the overheating of the lithium is significantly less than the surface overheating ($T/T_* \simeq 0.25$). This x section corresponds to a metastable state of liquid lithium; it is indicated by the point A in Figs. 3 and 1. Although the theoretical strength at this point is not reached, rupture of the liquid is very probable.

Negative pressures in the liquid metal can develop for large $Q\tau_p$ in the bulk of the layer only after the compression wave caused by the thermal shock reaches the second boundary $x = h$. Figure 4 shows an example of such a development of pressures in the liquid-metal layer, adjacent to an absolutely rigid wall; the thickness of the layer $h = 25l$, and the energy input corresponds to the value $Q\tau_p = 100$ ($Q = 10^4$, $\tau_p = 10^{-2}$). It is evident that by the end of the pulse (curve 1 — $\tau = 0.02$) a compression wave with an amplitude exceeding $50p_*$ forms near the surface; it propagates rapidly toward the wall (curve 2 — $\tau = 0.5$). Negative pressures appear in the layer when the reflected compression wave and the unloading wave interact (curves 3 and 4 — $\tau = 1.5$ and 2.8, respectively). The states corresponding to the points B and C in Fig. 4 are also indicated in Fig. 1; it turned out that the theoretical rupture strength of liquid lithium is reached in state B, while in the state C a pressure differing from the theoretical strength by only a factor of two is attained.

Thus rupture of the liquid in the bulk of the layer is practically unavoidable under the action of powerful radiation pulses on a liquid-metal shielding layer. We note that an increase in the thickness of the layer and a replacement of the boundary layer at the wall (1.7) by (1.6) has virtually no effect on the amplitude of the negative pressures developing in the layer.

LITERATURE CITED

1. A. P. Rybakov, "Study of the spallation fracture of condensed bodies," Zh. Prikl. Mekh. Tekh. Fiz., No. 5 (1981).
2. A. A. Kalmykov, V. N. Kondrat'ev, and I. V. Nemchinov, "Disintegration of an instantaneously heated material and determination of its equation of state from the value of the pressure and momentum," Zh. Prikl. Mekh. Tekh. Fiz., No. 5 (1966).
3. V. G. Volkov, K. G. Gainulin, et al., "Modeling of instantaneous thermal shock in a material with the help of relativistic electron beams," Voprosy Atomnoi Nauki i Tekhniki, Ser. Termoyadernyi Sintez, 1(7) (1981).
4. G. A. Carlson, "Dynamic tensile strength of mercury," J. Appl. Phys., 46, No. 9 (1975).
5. Yu. I. Arkhangel'skii, V. G. Volkov, et al., "Conditions of operation of structural materials in a pulsed thermonuclear reactor based on relativistic electrons beams," Voprosy Atomnoi Nauki i Tekhniki, Ser. Termoyadernyi Sintez, 1(3) (1979).

6. V. N. Kondrat'ev, I. V. Nemchinov, V. N. Pomerantsev, and V. M. Khazins, "Problem of motion in a two-dimensional layer of condensed material opposite to the flux of radiation taking into account evaporation and spallation," in: Advances in the Mechanics of Deformable Media [in Russian], Nauka, Moscow (1975).
7. Yu. V. Gott, Interaction of Particles with a Material in Plasma Research [in Russian], Atomizdat, Moscow (1978).
8. S. N. Kolgatin and A. V. Khachatur'yants, "Interpolation equations of state of metals," Teplofiz. Vys. Temp., 20, No. 3 (1982).
9. V. P. Skripov, The Metastable Liquid [in Russian], Nauka, Moscow (1972).
10. A. A. Samarskii and Yu. P. Popov, Difference Methods for Solving Gas-Dynamics Problems [in Russian], Nauka, Moscow (1980).

KINETICS OF SPALLATION RUPTURE IN THE ALUMINUM ALLOY AMg6M

G. I. Kanel', S. V. Razorenov,
and V. E. Fortov

UDC 532.593

It is well known that the magnitude of rupture stresses depends on the duration of the loads, but the quantitative expression for this dependence remains unclear. Under conditions of spallation, in the presence of very short actions, magnitudes of tensile stresses in metals approaching the values of the theoretical tensile strength are achieved, as reported, for example, in [1]. However, the method used in [1] to study spallation phenomena, based on an analysis of samples remaining after the tests, could significantly overestimate the values of the rupture stresses attained [2]. In this respect, the most reliable and informative method is the method of determining the spallation strength from continuous records of the velocity profiles of the free rear surface of the samples w(t). In this work, we measured the profiles w(t) and determined the magnitude of the spallation strength of the aluminum alloy AMg6M in a wide range of characteristic durations of incident loading pulses. Based on the data obtained, the previously proposed [3] continuous model of rupture is modified and the calculations using the proposed kinetics of rupture are compared with the experimental data.

The samples studied were prepared from sheets 1.8-10 mm thick. The transverse dimensions of the samples were equal to 80-120 mm. The one-dimensional compression pulses in the samples were generated by striking an aluminum foil 0.19-0.40 mm thick with a velocity of 675 $\pm$ 15 m/sec or by detonating an explosive (explosion lens) in contact with the sample. The foil was hurled with the help of explosion setups similar to those described in [2]. The velocity profiles of the free back surfaces of the samples were recorded continuously with the use of capacitative sensors [4]. Depending on the required resolution and recording time, the diameter of the measuring electrode was 5-20 mm, and the distance between the electrodes and the surface of the sample was 1-6 mm, respectively.

The recorded changes in the velocity of the sample surface w with time t are shown by the solid lines in Fig. 1, where each curve was obtained by averaging data from two to five experiments. The loading conditions are indicated in Table 1. The use of capacitive sensors with a diameter of 5 mm ensures that the rise time of the velocity of the surface at the front of the shock wave is resolved at a level of 10-15 nsec. For shock waves whose amplitude is lower than 3 GPa, the recorded rise time is much greater than this limit, which agrees with the results of measurements performed with the use of laser interferometry [5].

The emergence of an elastic precursor with an amplitude of 0.37 GPa, which corresponds to a dynamic yield stress of σ_T = 0.18 GPa, at the surface is clearly evident in the profiles w(t). The emergence of a plastic shock wave and the head part of the incident rarefaction

Chernogolovka. Translated from Zhurnal Prikladnoi Mekhaniki i Tekhnicheskoi Fiziki, No. 5, pp. 60-64, September-October, 1984. Original article submitted July 24, 1983.

0021-8944/84/2505-0707$08.50